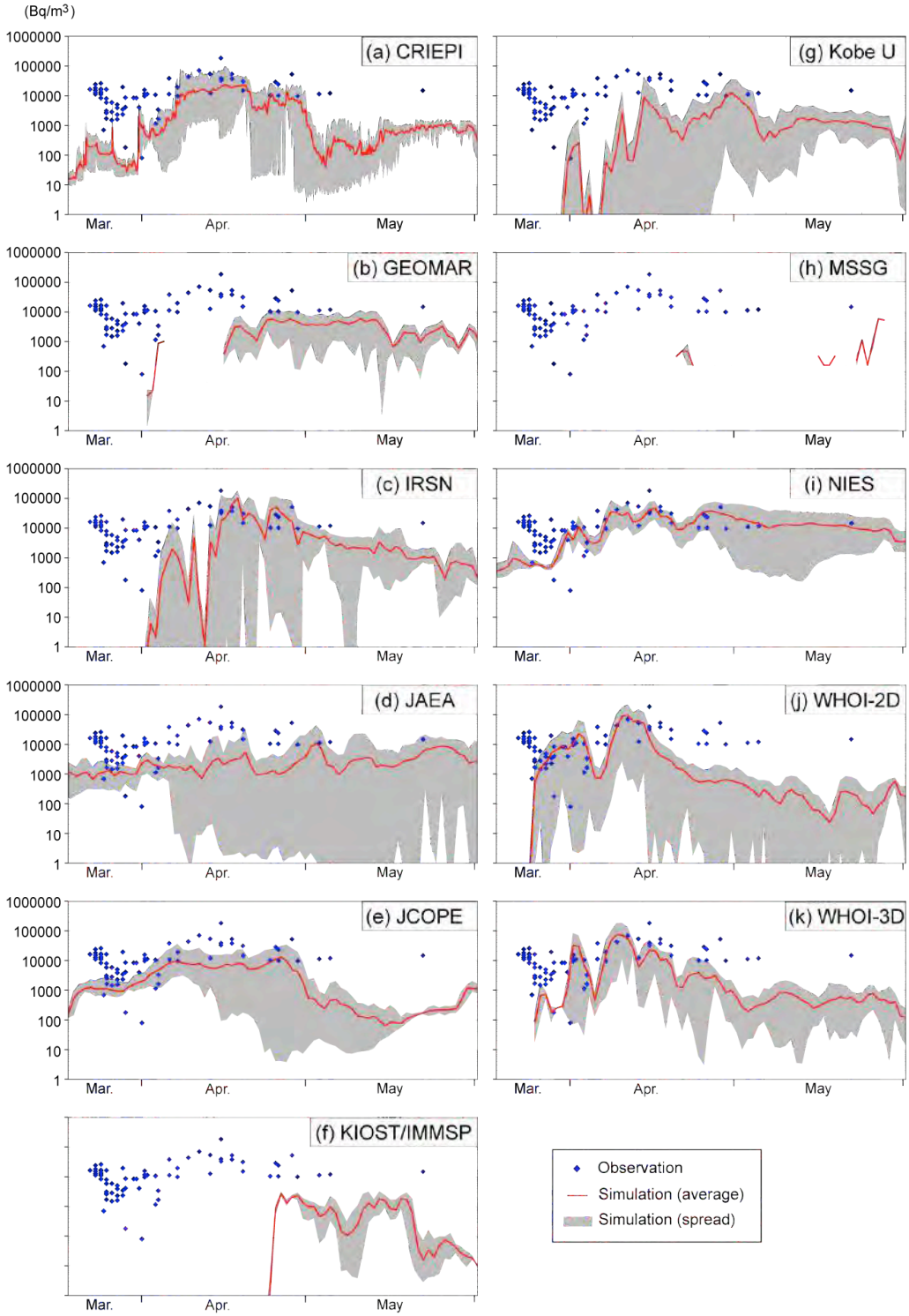

Figure 5.9. Time series of ^{137}Cs concentrations at the monitoring stations 30 km offshore of the FDNPP from March 18th to June 1st, 2011. The observed values from ten stations are indicated by blue solid diamonds. The simulated time series that was averaged over the locations of ten observation stations is shown by the red line. Gray shading indicates the spread of the time series at ten locations for each model.

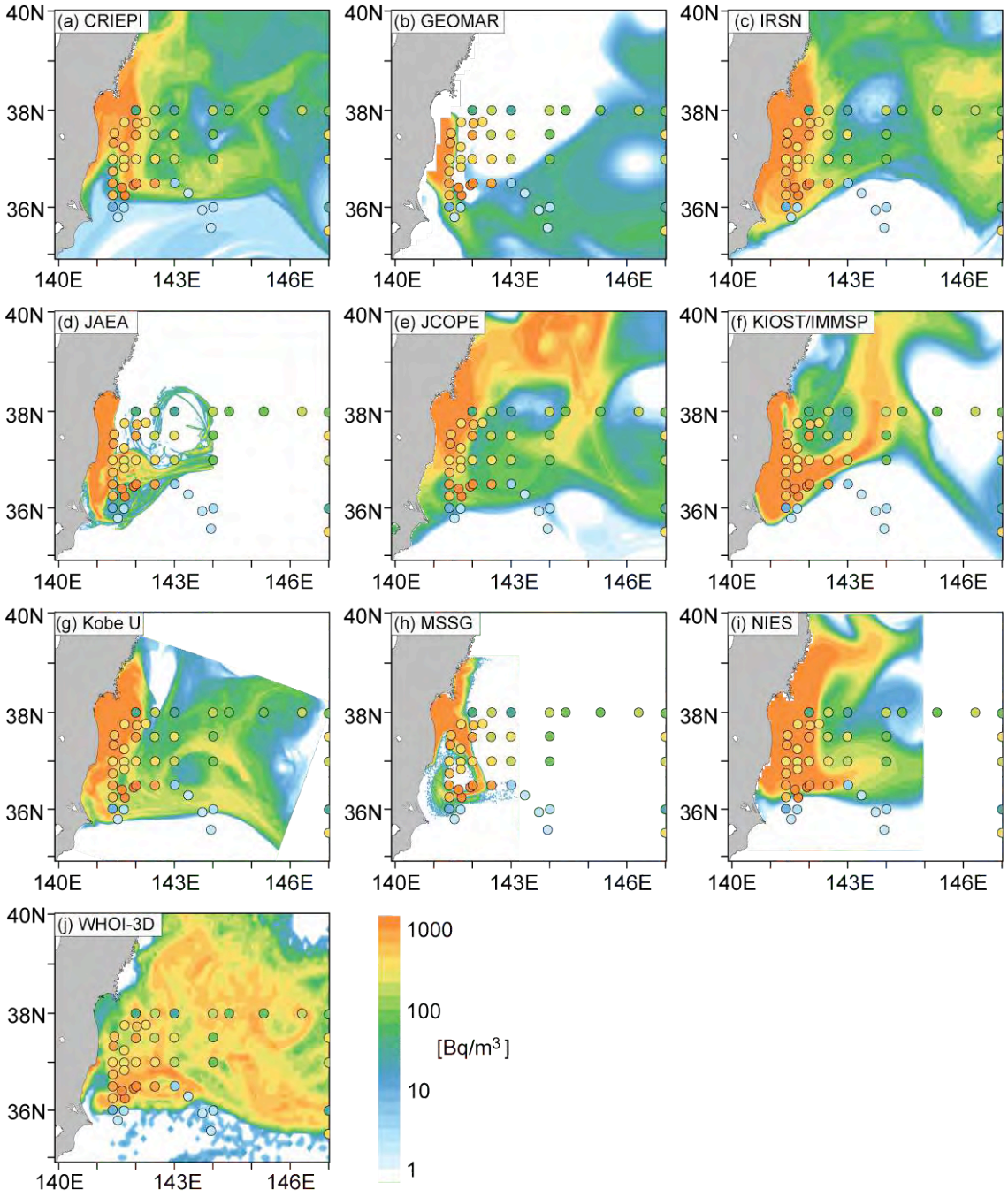

Figure 5.10. Horizontal distribution of surface ^{137}Cs concentrations averaged from June 8-18, 2011. The simulated distributions are shaded in color, and the observed values are indicated by circles with the same color-scale.

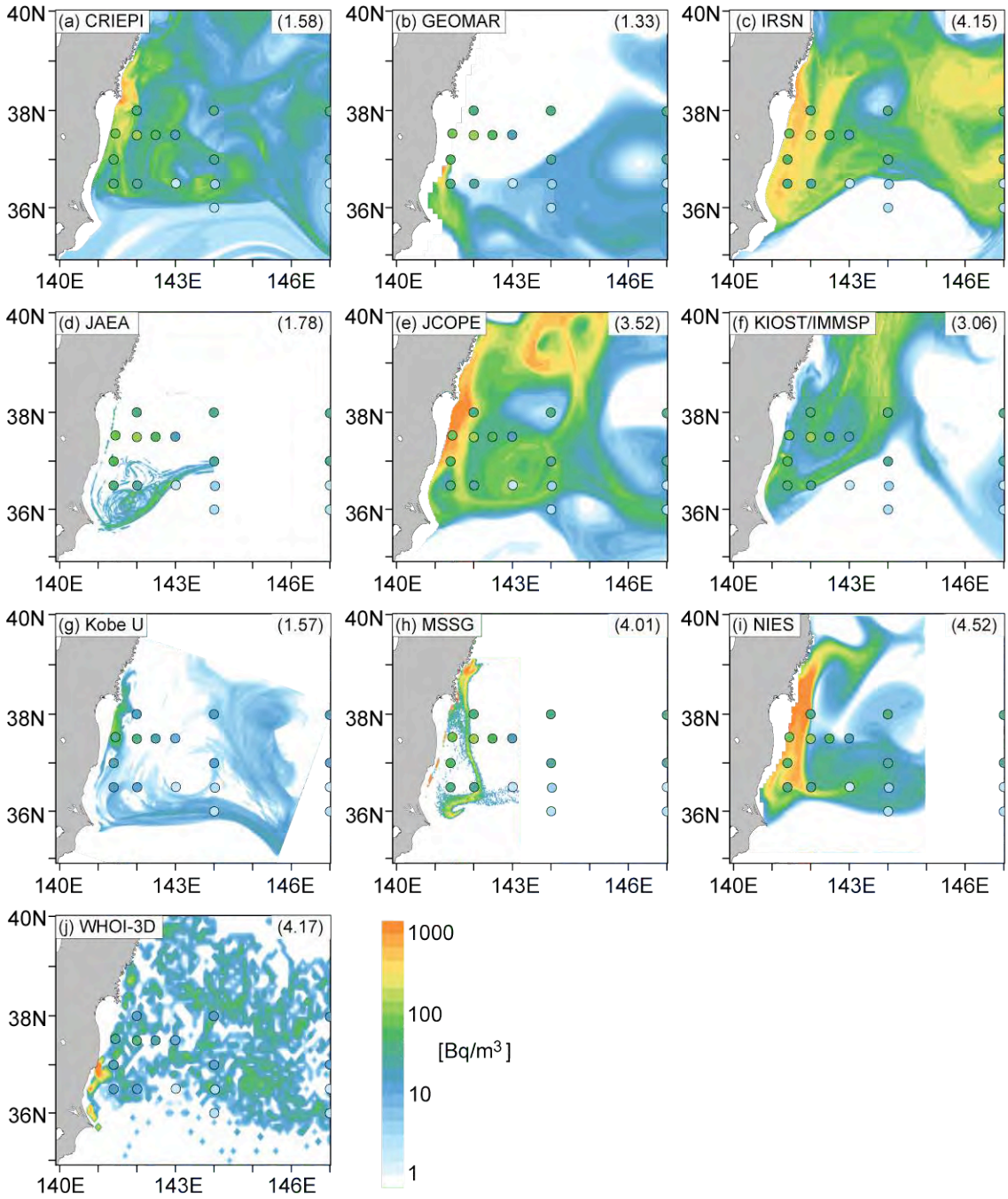

Figure 5.11. Same as in Fig. 5.10 except for at a depth of 100 m. Numbers in parentheses shown in the upper-right corner of each panel indicate the ^{137}Cs inventory within the R/V KOK observation area from the surface to a depth of 200 m. Unit for the inventory is in Peta Bq.

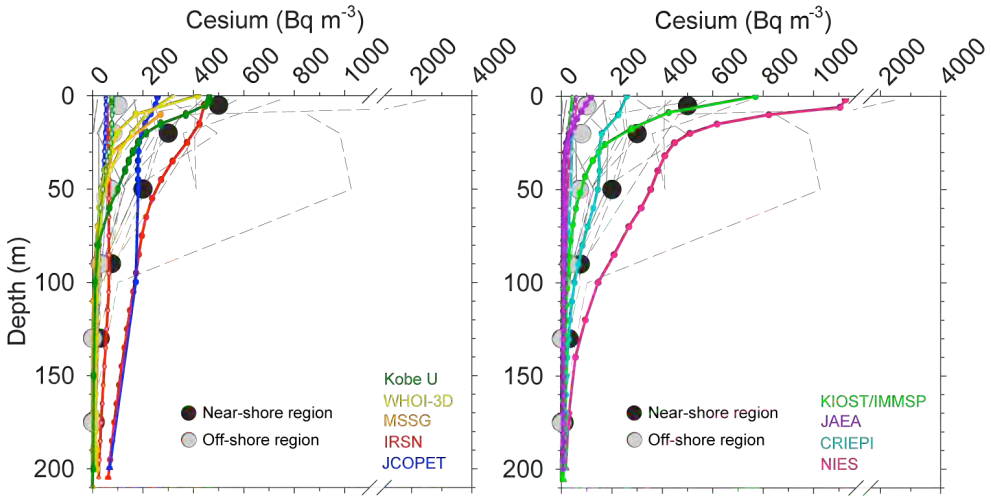

Figure 5.12. Vertical profiles of ^{137}Cs averaged over the area of the R/V KOK observations. Black and gray dots indicate the observed values of ^{134}Cs for the near-shore region and off-shore region, respectively (after Buesseler et al., 2012). The simulated vertical profiles for the near-shore region (lines with open circles) and off-shore region (lines with solid circles) are shown. The observed values for the left panel and right panel are the same except that the simulated profiles are from different models. Note that we compare the simulated profiles of ^{137}Cs to the observed values of ^{134}Cs because the only available profile in Buesseler et al., 2012 is for ^{134}Cs and because the ratios of concentrations between ^{134}Cs and ^{137}Cs in the study area are almost one in June.

6. Emission source estimation

6.1. Introduction

As described in the previous model inter-comparison sections, the results of the tracer transport simulations of the radionuclides varies significantly depending on the prior source term conditions. More than three years have passed since the accident at the Fukushima FDNPP; however, a robust source term estimation still has not been obtained. Chino et al. (Chino et al., 2011) from the Japan Atomic Energy Agency (JAEA) used a reverse method in which they compared radionuclide observational data and their regional tracer transport model (SPEEDI) simulation results to obtain the emission time series of ^{137}Cs and ^{131}I. Their results suggested that the ^{137}Cs total emission amount from the FDNPP for the period of March 11 - April 19 is 9.1 PBq and that the maximum emissions occurred from March 14 and 15 (Chino et al., 2011). They also found that there were large emission events at March 21-22 and March 30-31. Terada et al. (2012) modified this result and obtained a ^{137}Cs total emission of 8.8 PBq. An important condition of their analyses was that only Japanese land observation sites were used; therefore, they could not constrain the radionuclide plumes that were transported to the Pacific Ocean. However, Stohl et al. (2012) combined a tagged tracer global tracer transport model (FLEXPART) results and observation data from the global radionuclide monitoring network operated by a preparatory commission for the Comprehensive Nuclear-Test-Ban Treaty Organization (CTBTO) through a Bayesian synthesis inversion (Maki et al., 2011). Stohl et al.'s results suggested that the total ^{137}Cs estimation in the period was 36.6 PBq. The result was a factor of 4 larger than the result by Chino et al. (2011) and Terada et al. (2012). Their analysis assessed the radionuclide plumes that were transported to the Pacific Ocean because they used widely covered observation data in the Northern Hemisphere and global transport model. However, Stohl et al.'s transport model is a Lagrangian transport model, and they released a large amount of tracer particles to simulate their transport, diffusion and deposition processes. The Lagrangian models have features that can precisely calculate transport processes; however, they cannot estimate diffusion (turbulent, cumulus and planetary boundary layers) and deposition (wet and dry) processes in detail. Such features might affect their diffusion and deposition processes, which are the most important processes in the long-range aerosol tracer transport. In this section, a new estimation of the ^{137}Cs source term is shown by combining the global observation network data, global Eulerian aerosol transport model and Bayesian synthesis inversion

(Maki et al., 2011).

6.2. Analysis Method

The present method used tagged simulation results by the global Eulerian aerosol model MASINGAR (Tanaka et al., 2005) in which the horizontal resolution was TL319 (approximately 60 km). Tagged tracers (^{137}Cs) from the lowest model layer (surface to 50 m) were released every three hours with 1Tg/hr to accumulate the daily mean. It was assumed that the released ^{137}Cs was attached to hydrophilic aerosols that had radii of 0.7 μm and occurred by dry and wet deposition. One of the merits in using tagged tracer simulations was that after the^{137}Cs source term emission time-series were obtained, we could also obtain the atmospheric concentrations and depositions of ^{137}Cs by simply calculating the linear combination of the source term estimations and tagged tracer simulation results. Using this feature, we could construct a near-real-time prediction system by combining the properly distributed observation network and operational system of the tagged tracer transport model (an emission prediction scenario is required when using such a system operationally). The daily mean observation data of 51 global sites (CTBTO(Hoffmann et al., 2000), RING OF FIVE(Masson et al., 2011)、University of California(Smith et al., 2014, Taiwan Academia Sinica(Hsu et al., 2012) and Meteorlogical Research Institute (Igarashi et al., 2009)) were collected (Fig. 6.1), and the analysis period was the 40 days from March 11 to April 19. We tested two prior emission estimates. The first estimate was the JAEA posterior emissions (Terada et al., 2012) and the second was the NILU prior emission (not posterior) (Stohl et al., 2012) because our observational data were similar to the data from their study. To consider the observational error and space representational error, the observational error was set to 20%. The prior flux uncertainty shows the ratio between the observation and prior flux uncertainty, and several sensitivity tests were examined by changing the prior emission flux uncertainties from 10% to 5000%.

6.3. Results and discussion

We selected the Stohl's source term estimation (Stohl et al., 2012) as our prior emission to compare the mismatch between observation data and estimated concentration. We also set the prior flux uncertainty to 100% after several sensitivity tests. The total ^{137}Cs emission amount from the FDNPP for the period of March 11 to April 19 was 19.4 PBq, and its

uncertainty was estimated as 3.6 PBq. In the present inverse analysis, the emission height level did not have as much of an affect in the estimated time-series of the source term. The maximum ^{137}Cs occurred on March 15 and the emission amount was larger than that of the prior estimates. The results suggest that there were emission events from March 18-22 and from March 28-30 (Fig. 6.2); however, the 28-30 March emission amount was smaller than that of the Chino et al. and Terada et al. estimation.

In our analysis, we obtained an intermediate result between that of Stohl et al. (2012) and Terada et al. (2012) using tagged tracer simulation results, global observation data and an inverse model, and the results were consistent with other analysis results (Table 6.1). By combining this result and the tagged simulation results, the atmospheric concentrations and deposition estimates of ^{137}Cs were evaluated. However, there are several issues to be discussed in the analysis. One of the most important issues is that we used only one model, and the bias of the model transport could directly affect the estimated source term. To obtain a robust source term estimation, we should collect many tagged model simulation results with common experimental settings and compare their estimated source terms. Another issue is the horizontal resolution of the model. To obtain a fine horizontal and temporal resolution, we should use a regional chemical transport model and collect hourly observation data. Currently, we do not have enough observation data for the Pacific Ocean; therefore, we should make use of marine deposition observation data to improve the analysis.

Table 6.1. Recent ^{137}Cs source term estimations from the FDNPP.

References	Total flux F_A	Range	To- F_A ratio of land deposition of 2.65PBq (%)	Period	Remarks
This study	19.4	16.4–22.4	13.7	3/11–4/19	Cs137 conc.; Global Eulerian model + Inversion
MEXT (2011) and Chino et al. (2011)	15.5	14–17	17.1		From obs. and numerical model analysis
Kobayashi et al. (2013)	13.0	–	20.4	3/12–3/20	Cs137 conc and sea surface conc.; Regional Lagrangian model, oceanic dispersion simulation + Reverse method
Saunier et al. (2013)	15.5	–	17.1	3/11–3/27	Gamma dose ratio obs.; Regional Eulerian model + Inversion.
Stohl et al. (2012)	36.6	20.1–53.1	7.2	3/10–4/20	Cs137 conc.; Global Lagrangian model + Inversion
Terada et al. (2012)	8.8	–	30.1	3/10–3/31	Cs137 conc.; Regional Lagrangian model + Reverse method
Winiarek et al. (2014)	15.5	11.6–19.3	17.1	3/11–3/26	Cs137 conc and sea surface deposition; Regional Eulerian model + Inversion.
mean±standard deviation(σ)	17.8 ±8.2		17.5±6.4		
data within 2σ from the mean	14.6±3.2		19.2±5.2		

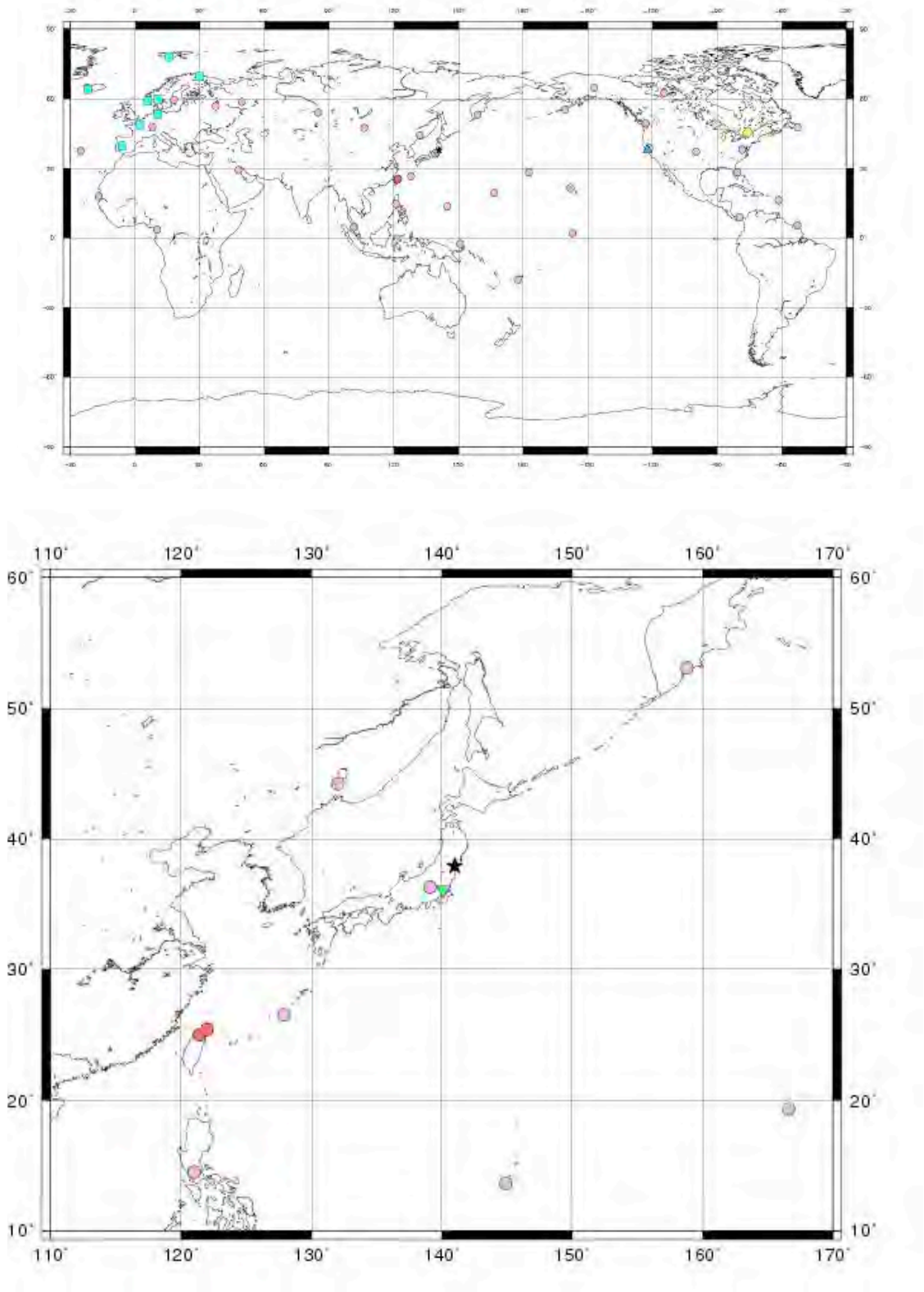

Figure 6.1. Observation data used in this study. Red, green and blue circles show the CTBTO, Ro5 and other observation data, respectively.

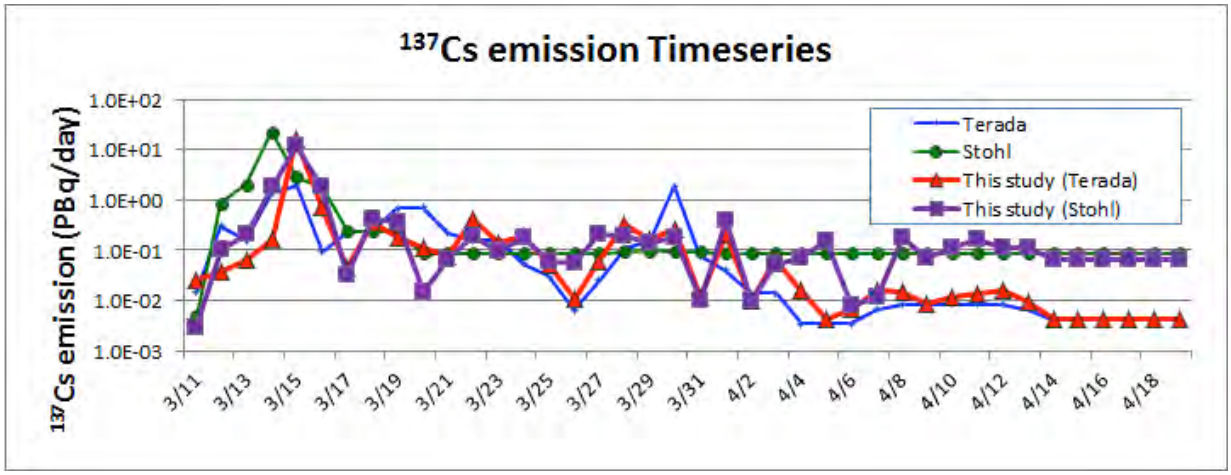

Figur 6.2. ^{137}Cs emission time series from the FDNPP Blue, orange, red (thick) and purple (thick) lines show the Terada prior, Syohl prior, inversed posterior (Terada prior) and inversed posterior (Stohl prior) ^{137}Cs emission time series, respectively.

7. Summary and concluding remarks

A summary of findings from past studies and the current study are presented below:

- JMA model estimate of the amount of ^{137}Cs released to the atmosphere until the end of March 2011 is 19.4±3.0 PBq. The estimate including results of the past studies is 17.8±8.2 PB (Table 6.1). The estimate only with values within twice the standard deviation around the mean value is 14.6±3.2 PBq.

- The amount of direct discharge to the ocean is estimated in the range of 2.3 to 26.9 PBq.

- Regional atmospheric model results show that the land area deposition ratio to the total emission is 27±10% (Table 3.2). On the other hand, the MEXT aircraft observation on May 31, 2012 shows a deposition of 2.7 PBq over the land. This observed value and the estimated total emission in each model lead to a land area deposition ratio of 18±6% in average. The value becomes 19±5% if the total emission within twice the standard deviation is use for evaluation. The differences are caused by errors in model simulation, estimation of the total emission, and estimation of the land-dopositted amount from the aircraft observation. We need future investiation to reduce the erros.

- The global atmospheric model comparison indicates that the wet doposition over the globe is 93±5% of the total ^{137}Cs emissions assumed in the models. The regional atmospheric model comparison, on the other hand, shows that the ratio over the simulation regions is 68±19%. The ratio over the Japanese land area is similar to this value. The difference between ratios of global and regional simulations is mainly caused by difference in the model regions, but model differences are also not negligible.

- Models are capable of depicting the main features of observed radioactive material distributions. There are, however, large uncertainties in the quantitative comparisons of the simulation results, especially in the amount of wet deposition, which is largely dissimilar in the different models. In addition, the eddy simulations in the coastal oceans have large differences between models.

- Migrating atmospheric pressure systems frequently change the wind direction and vertical shear; therefore, the simulated distributions of the deposition patterns over the land and ocean are sensitive to the assumed meteorological data and emission scenarios. Accurate and high temporal resolution scenarios must be reconstructed through future efforts of extensive assimilation and inversion.

- Estimates of depositions to the ocean through atmospheric fallout and direct discharge are required to reproduce the observed ^{137}C concentrations in the ocean. The atmospheric deposition of ^{137}Cs to the ocean is underestimated before mid-April. It is, therefore, needed to improve the deposition of radioactive materials from atmosphere to ocean for improved simulation of ocean transport of the materials.

- The skill of the models depends on the performance of the dynamic frameworks, chemical transportation processes, dry and wet deposition processes and other elements. Therefore, significant improvements can be made to the models through collaborative works among different communities.

- The estimated emission scenarios by local and global analyses are different; therefore, a combined inversion analysis with both local and global data is required. Therefore, the work shown in Chapter 6 must be extended to include high spatial resolution inversions using regional models.

Acknowledgments

We cordially acknowledge all of the individuals and organizations that provided contributing results and related information for the present report. Acknowledgements are extended to all those whose efforts assisted in the publication of this report.

Appendix

Appendix 3A. Model description for regional atmospheric model intercomparison

3A.1. Centre d'Enseignement et de Recherche en Environnement Atmosphérique (CEREA)

The simulations of the radionuclides from the FDNPP were performed with the chemistry transport model Polar3D, which is the Eulerian model of the Polyphemus platform; this model has been validated by the European Tracer Experiment, Algeciras incident and Chernobyl accident (Quélo et al., 2007).

^{137}Cs and ^{131}I are modeled as passive gaseous tracers with radioactive decay, and their half-lives are 11,000 and 8.04 days, respectively. Dry deposition is modeled using a simple scheme with a constant deposition velocity: v^{dep} = 0.2 cm s^{-1} for ^{137}Cs and v^{dep} = 0.5 cm s^{-1} for ^{131}I. The wet scavenging rate Λ^s used in this study is based on Brandt et al.(2002). The advection is implemented by a third-order direct space-time scheme with a Koren-Sweby flux limiter function. Because of the sharp gradients, such a limiter should be used. The diffusion scheme is integrated through an implicit second-order Rosenbrock scheme that has a three-point spatial scheme and directional splitting. The model is configured with a spatial resolution of 0.05° (270×260 grids) and 15 vertical levels ranging from 0 to 8000 m.

The initial source terms for ^{137}Cs and ^{131}I were obtained by inverse modeling of active concentrations in the air at the mesoscale using a rigorous estimation of the error level (Winiarek et al., 2012). A finer source term for ^{137}Cs was obtained by inverse modeling of several datasets that included the active concentrations in the air and the deposition measurements; a rigorous estimation of the errors was attached to each dataset (Winiarek et al., 2014). For the first estimation, the ECMWF meteorological fields were used; they were available every 3 h at a spatial resolution of 0.25°×0.25° using the mesoscale meteorological model WRF. Using the parameterizations described in Winiarek et al. (2014), fields were generated every hour with a spatial resolution of approximately 0.05°× 0.05°.

3A.2. Central Research Institute of Electric Power Industry (CRIEPI)

A modeling group from the CRIEPI simulated radionuclides using the Comprehensive Air Quality Model with Extensions (CAMx) version 5.40.1 (ENVIRON, 2011) that was driven by WRF version 3.2.1 (Grell et al., 2005). The chemical module of the CAMx was modified to analyze the advection, diffusion, radioactive decay, and dry and wet deposition of gaseous and particulate ^{131}I and particulate ^{132}I, ^{132}Te, ^{134}Cs and ^{137}Cs. The particulate radionuclides were assumed to be equivalent to $PM_{2.5}$ (particulate matter < 2.5 μm). The model domain covered the east side of Japan with 5-km grids, and the model had 34 layers up to 100 hPa. The wet deposition process, which was originally based on Seinfeld and Pandis (1998), was modified to analyze the vertical re-distribution of radionuclides by precipitation. The dry deposition process was based on Zhang et al. (2001) and Zhang et al. (2003) for particulate and gaseous radionuclides, respectively. The objectively analyzed dataset (MANAL) constructed by the JMA was used as the lateral boundary and initial condition for the WRF. Analysis nudging using MANAL was applied for the meteorological field during the simulation. The release rates of ^{131}I and ^{137}Cs were from Terada et al. (2012).

3A.3. Institut de Radioprotection et Sûreté Nucléaire (IRSN)

The atmospheric transfer modeling group from the IRSN simulated radionuclide dispersion using the Eulerian model ldX that was derived from PLAIR 3D. The simulation submitted to the working group was driven by the meteorological fields from the JMA forecast (0.05°×0.05°). The source term used here was described in Mathieu et al. (2012). Built in 2011, this source term was mostly based on the analysis of the dose rate measurement to determine doses that may have been taken during the catastrophe. The dry deposition model was based on a deposition velocity value of 2×10^{-3} m s^{-1} for aerosols. The wet deposition was modeled by a scavenging coefficient $L=L_0P$, where P is the precipitation (mm h^{-1}) read from the ECMWF fields, and L_0 is a constant defined per radionuclides (aerosols: 5×10^{-4} h s^{-1} mm^{-1}). The details for this model are described in Korsakissok et al. (2013), and the revised release rate using this model can be found in Saunier et al. (2013).

3A.4. Japan Atomic Energy Agency (JAEA)

The WSPEEDI model (Terada et al., 2008) was constructed by expanding the function of SPEEDI with a combination of the non-hydrostatic mesoscale atmospheric model MM5

(Grell et al., 1994) and Lagrangian particle dispersion model GEARN (Terada and Chino, 2008). The MM5 is a community model that has users all over the world, and it is used as the official weather forecast by some countries. It has many useful functions, such as nesting calculations and 4-D data assimilation, and numerous options for parameterizations for cloud microphysics, cumulus clouds, the planetary boundary layer (PBL), radiation, and land surface schemes. The Lagrangian particle dispersion model GEARN calculates the atmospheric dispersion of radionuclides by tracing the trajectories of a large number (typically a million) of marker particles discharged from a release point. The horizontal model coordinates are the map coordinates, and the vertical coordinates are the terrain-following coordinates (z*-coordinates). By using the meteorological field predicted by the MM5, the GEARN model calculates the movement of each particle affected by the advection from the mean wind and subgrid-scale turbulent eddy diffusion. The GEARN model also has a function of nesting calculations for two domains corresponding to the MM5 nested domains. Two nested domains of the GEARN model are calculated concurrently by different executables on parallel computers, and the marker particles that flow out and in across the boundary of the inner domain are exchanged between domains. Part of the radioactivity in the air is deposited on the ground surface by turbulence (dry deposition) and precipitation (wet deposition). The decrease in radioactivity that results from dry deposition is calculated for each particle using the dry deposition velocity (0 m s^{-1} for noble gases, 3×10^{-3} m s^{-1} for iodine, and 10^{-3} m s^{-1} for other nuclides, which does not consider the chemical form and particle size) based on the typical value for short vegetation (Sehmel, 1980). The decrease in radioactivity of each particle by wet deposition is calculated by the scavenging coefficient that is calculated at each grid cell for any nuclides except for the noble gases and is based on the precipitation intensity for convective and non-convective rains predicted by the MM5. The scavenging coefficient (Λ) based on the study by (Brenk and Vogt, 1981) is calculated at each grid cell for any nuclides except for noble gases in the GEARN model as

$$\Lambda = \alpha\left(F_c I_c + F_n I_n\right)^{\beta}$$

where α ($=5\times10^{-5}$) and β ($=0.8$) are the empirical constants, and I_c and I_n are the precipitation intensities ($mm\ h^{-1}$) for convective and non-convective rains, respectively, that are predicted by the MM5. F_c and F_n are the unity at grid cells below the convective and non-convective

cloud heights, respectively; the value is zero at other grid cells. The air concentration in each Eulerian cell averaged over an output time interval and total surface deposition accumulated during the time interval are calculated by summing the contributions of each particle to the cell. The radioactive decay is calculated at each time step and integrated into both the air concentration and surface deposition calculations, although the decay chains are not considered. The radiological doses are calculated by multiplying the air concentration and deposition by conversion factors (ICRP, 1995). The performance of this model system was evaluated by its application in the field tracer experiment over Europe, ETEX (Furuno et al., 2004) and the Chernobyl nuclear accident (Terada et al., 2004; Terada and Chino, 2005; 2008).

3A.5. Japan Agency for Marine-Earth Science and Technology (JAMSTEC)

A modeling group from the JAMSTEC simulated the radionuclides using the Weather Forecast and Research (WRF) model with an online chemical module (WRF/Chem) version 3.4.1 (Grell et al., 2005). The chemical module of WRF/Chem was modified to analyze the advection, diffusion, and dry and wet deposition of ^{131}I and ^{137}Cs. The model domain covered the east side of Japan with 3-km grids, and the model had 35 layers up to 100 hPa. The wet deposition process was based on Maryon et al. (1996), and the dry deposition process was based on Maryon et al. (1992) and Klug (1992) for ^{131}I and ^{137}Cs, respectively. The mesoscale model (MSM) dataset constructed by the Japan Meteorological Agency (JMA) was used as the lateral boundary and the initial condition. Analysis nudging using the JMA-MSM and observational nudging with ground-based observations by the JMA was applied for the meteorological field during the simulation. The release rates of ^{131}I and ^{137}Cs were taken from Terada et al. (2012).

3A.6. Japan Meteorological Agency (JMA)

The Japan Meteorological Agency (JMA) provided its operational mesoscale (MESO) analysis, radar/rain gauge-analyzed precipitation (RAP) data, and simulated results from the JMA Regional Atmospheric Transport Model (JMA-RATM) in a collaboration with the WMO task team that was convened by the request of the United Nations Scientific Committee on the Effects of Atomic Radiation (UNSCEAR). The JMA-RATM is a tracer

transport model that can be driven by the MESO analysis. The model applies a Lagrangian scheme (Iwasaki et al., 1998; Seino et al., 2004) with many tracer particles that follow advection, horizontal and vertical diffusion, gravitational settling, dry deposition and wet scavenging processes. The JMA-RATM was originally developed at the JMA for photochemical oxidant predictions (Takano et al., 2007) and volcanic ash fall forecasts (Shimbori et al., 2009) in Japan. The details of the original RATM were described by Shimbori et al. (2010).

For the prediction of radionuclides, the implementation of dry and wet deposition schemes were improved. Regarding the wet deposition for light particles, only washout processes (below-cloud scavenging) were considered. The below-cloud scavenging rate was from Kitada (1994). The grain size distribution assumed a lognormal with a mean diameter of 1 μm, standard deviation of 1 (upper cutoff of 20 μm), and a uniform particle density of 1 g cm^{-3}. Calculations of the JMA-RATM were conducted according to the WMO task team's agreed upon protocol with a horizontal concentration and deposition grid resolution of 5 km using a unit source emission rate (Draxler et al., 2013). For the SCJ model intercomparisons, the revised JAEA release rate by Kobayashi et al. (2013) was used, and the time step of Lagrangian trace calculations was changed to 5 minutes from the original of 10 minutes. In addition, the precipitation rate of solid water (snow and graupel) in the JMA-MESO analysis was used for wet scavenging in addition to that of rain. The details of the revised JMA-RATM are described in Saito et al. (2014).

3A.7. Meteorological Research Institute, Japan Meteorological Agency (JMA-MRI)

We used the Regional Air Quality Model 2 (RAQM2; Kajino et al. (2012), Adachi et al. (2013), which implements a triple-moment modal aerosol dynamics module assuming a log-normal size distribution of the aerosol populations. This model describes the nature of the aerosol dynamic processes, such as nucleation, condensation, coagulation, dry deposition, grid-scale cloud condensation and ice nuclei activation, and the subsequent cloud microphysical processes (rainout) and washout processes. An ensemble Kalman filter (EnKF) data assimilation system coupled with the JMA non-hydrostatic meteorological model (NHM-LETKF) (Kunii, 2013) was used to produce the meteorological field. There were 213 × 257 grids with a 3-km horizontal grid resolution in the NHM-LETKF and RAQM2. There were 50 vertical layers to 50 hPa in the NHM-LETKF and 20 layers to 10 km in the RAQM2.

For the radioactive aerosols, we used a number equivalent to the geometric mean dry diameter $D_{g,n,dry}$ = 100 nm, geometric standard deviation σ_g = 1.3, particle density ρ_p = 2.0 g cm^{-3}, and hygroscopicity κ = 0.4 (internal mixture with sulfate and others assumed). We assumed I_2 for the chemical composition of gaseous iodine. When emitted, 20% and 80% of ^{131}I are assumed to exist in the gas and aerosol phases, respectively. The release rates of ^{131}I, ^{137}Cs, and ^{134}Cs were from Terada et al. (2012).

3A.8. National Institute for Environmental Studies (NIES)

A modeling group from the NIES simulated the distributions of ^{137}Cs using WRF version 3.1 (Skamarock et al., 2008) and the three-dimensional chemical transport model Models-3 Community Multiscale Air Quality (CMAQ) (Byun and Schere, 2006) for the period from March 10 to April 20 2011. The deposition schemes used in the CMAQ were detailed in Byun and Ching (1999) and Byun and Schere (2006). The dry deposition was simulated using a resistance model. The cloud module of the CMAQ includes parameterizations for sub-grid convective precipitating and non-precipitating clouds and grid-scale resolved clouds. They assumed that all of the ^{137}Cs were in the particulate phase with a diameter of 1 μm (Sportisse, 2007). The model domain covered most of the Tohoku region (711 × 711 km^2) at a 3-km grid resolution and 34-layer vertical structure with a surface layer thickness of approximately 60 m. For the WRF simulation, analysis nudging was conducted with the three-dimensional meteorological fields from the Japan Meteorological Agency Meso-Scale Model datasets that had 5 × 5 km^2 horizontal resolution for 3-h intervals. The emission data from the FDNPP were from Terada et al. (2012).

In CMAQ, the wet scavenging of particulate matter is calculated by the following equation:

$$\frac{dQ_i}{dt} = Q_i\left(\frac{\exp\left(-\tau_{cld}/\tau_{washout}\right)-1}{\tau_{cld}}\right) \quad \text{(S1)}$$

where Q_i is the in-cloud concentration of pollutant i, τ_{cld} is the cloud timescale, and $\tau_{washout}$ is the washout time calculated from

$$\tau_{washout} = \frac{W_T \Delta z}{\rho_{H2O} p_0} \quad \text{(S2)}$$

where W_T is the mean total water content, Δz is the cloud thickness, ρ_{H2O} is the density of water, and p_0 is the precipitation rate (mm hr^{-1}).

3A.9. Seoul National University (SNU)

The Eulerian transport model (ETM) was obtained from a modification of the Asian Dust Aerosol Model 2 (ADAM2) (Park et al., 2010). The ADAM2 model used 11 particle-size bins with nearly the same logarithmic intervals for the particles with radii of 0.1-37 μm, and it was adapted to a logarithmic size distribution with an aerodynamic mean diameter of 0.4 μm and a logarithmic standard deviation of 0.3 for ^{137}Cs (Stohl et al., 2012) For ^{131}I, the ADAM2 model was adapted to handle the gas phase contaminants. The horizontal resolution of the ETM was 27 km, which was the ETM domain centered by the FDNPP. The meteorological model used in this study was the fifth-generation mesoscale model of the non-hydrostatic version (MM5; Grell et al. 1994). The wet deposition amounts of radionuclides were determined by the precipitation rate, and the average concentration in the cloud water was estimated by the sub-grid cloud scheme followed by the diagnostic cloud model in the ADAM2 and the Regional Acid Deposition Model (RADM) version 2.6 (Chang et al., 1987). The below-cloud scavenging process was also included (Park, 1998). The emission rate of ^{131}I and ^{137}Cs from the accident at the FDNPP by JAEA (Chino et al., 2011; Katata et al., 2012) was used. The details of the ETM can be found in Park et al. (2013).

Appendix 4A. Model descriptions for global atmospheric model intercomparison

4A.1. SPRINTARS

SPRINTARS (Spectral Radiation-Transport Model for Aerosol Species) (Takemura et al., 2000; Takemura et al., 2002; Takemura et al., 2005) is a global aerosol model developed by the Research Institute for Applied Mechanics, Kyushu University. The model simulates the effect of atmospheric aerosols on climate systems and atmospheric pollution over a global scale. The model is based on the atmosphere-ocean coupled climate model MIROC, which was developed by the Atmosphere and Ocean Research Institute, University of Tokyo, National Institute for Environmental Studies, and the Japan Agency for Marine-Earth Science and Technology (Watanabe et al., 2010).

SPRINTARS calculates the transport processes of aerosols (emission, advection,

diffusion, wet deposition, dry deposition, and gravitational settling). The aerosol direct effect, which is caused by the scattering and absorption of solar and terrestrial radiation by aerosols, and the indirect effect, which is an act of aerosols as cloud condensation nuclei and ice nuclei, are included in the calculation. SPRINTARS is the only aerosol model from the Asian research community that was adopted by the 4th assessment of the Intergovernmental Panel on Climate Change (IPCC). In June 2011, Takemura et al. (2011) published a simulated result of the global transport of a tracer from the FDNPP just after the accident. The horizontal resolution of the model is approximately 0.56° × 0.56° in latitude and longitude (T213 spectral truncation in the dynamical core), and the model has 20 vertical layers up to 8 hPa, including 4 layers below an altitude of 1 km (approximately at the 50, 200, 500 and 1000-m levels). The horizontal wind field components and air temperature internally generated by the dynamical core are nudged by 6-hourly NCEP GFS data.

In the intercomparison study, simulations of ^{137}Cs, ^{131}I and ^{133}Xe have been submitted. The dry and wet deposition parameterizations of ^{137}Cs and ^{131}I were the same as sulfate aerosol, whereas ^{133}Xe was assumed to be only removed by the radioactive decay. The source terms of ^{137}Cs and ^{131} I were from the estimated values by the JAEA (Terada et al., 2012). For the ^{133}Xe experiment, the inversely estimated source term of Stohl et al. (2012) was used. Two sets of the experiment, namely the standard experiment, “SPRINTARS,” and an experiment with stronger wet deposition parameters “SPRINTARS1,” were submitted to the intercomparison.

4A.2. MASINGAR-1 and MASINGAR mk-2

MASINGAR (model of aerosol species in the global atmosphere) is a global aerosol model developed by the Meteorological Research Institute of Japan Meteorological Agency. For the intercomparison, the simulated results with two versions of the model were submitted. MASINGAR-1 was coupled with an AGCM called the MRI/JMA 98, which has been used as the operational dust forecasting model by the Japan Meteorological Agency (JMA) since January 2004 (Tanaka et al., 2003). The model resolutions were set to a T106 Gaussian horizontal grid (approximately 1.125° × 1.125°) and 30 vertical layers from the surface to a height of 0.4 hPa. A newer version of this aerosol model called the MASINGAR mk-2 was coupled with an AGCM called the MRI-AGCM3 as a component of the earth system model of the Meteorological Research Institute, MRI-ESM1 (Yukimoto et al., 2011; Yukimoto et al., 2012), and used as the global aerosol model for the CMIP5 climate change experiment. The

model resolutions were set to a TL319 horizontal grid (approximately 0.5625° × 0.5625°) and 40 vertical layers from the ground surface to a height of 0.4 hPa.

In this intercomparison experiment, the horizontal wind fields were assimilated with the six-hourly 1.25° ×1.25° data of the JCDAS global reanalysis (Onogi et al., 2007) with the Newtonian relaxation nudging technique. The JCDAS reanalysis was also used for the sea-surface temperature data. The released ^{137}Cs was assumed to be readily attached to the ambient aerosols, which had a uni-modal lognormal distribution with a mode radius of 0.07μm and a dispersion of 2.0 (Tanaka et al., 2013).

For the intercomparison, the simulated results of ^{137}Cs with the source terms of the JAEA (Terada et al., 2012) and Stohl et al. (2012) were submitted. For the ^{133}Xe experiment, the inversely estimated source term of Stohl et al. (2012) was used.

4A.3. EMAC

The simulations by the Cyprus Institute were conducted using the global atmospheric chemistry model EMAC (the ECHAM/MESSy Atmospheric Chemistry) version 1.9 (Christoudias and Lelieveld, 2013). The dynamical field of this model was calculated by the fifth generation European Centre Hamburg general circulation model (ECHAM5; Roeckner et al., 2003; 2006) version 5.3. The simulations were conducted with horizontal resolutions of T255 (approximately 0.5° × 0.5°) and T106 (approximately 1.125°× 1.125°). The vertical coordinate was a hybrid, and the number of vertical layers was 31 up to 10 hPa. The large-scale component of the model circulation dynamics was nudged by applying a Newtonian relaxation towards the European Centre for Medium-range Weather Forecasts (ECMWF) ERA-Interim reanalysis data (Simmons et al., 2007). The nudged variables were vorticity, divergence, temperature and surface pressure. The ERA-Interim data were used for dynamics only; therefore, the precipitation was model-generated.

For the intercomparison, the simulated results of ^{137}Cs, ^{131}I, and ^{133}Xe were submitted. The source terms of ^{137}Cs estimated by the JAEA (Chino et al., 2011) and Stohl et al. (2012) were used. For the ^{133}Xe experiment, the inversely estimated source term of Stohl et al. (2012) was used.

4A.4. KNMI TM5

The Royal Netherlands Meteorological Institute (KNMI) participated in the model

intercomparison of the transport of the radionuclides using the global chemistry Transport Model, version 5 (TM5) (Huijnen et al., 2010; Krol et al., 2005). TM5 is a global offline transport model that has been applied for many atmospheric chemistry and aerosol studies (e.g., de Meij et al., 2006; Vignati et al., 2010) and chemical weather and climate simulations, in which TM5 is driven by ERA-Interim data or the Integrated Forecasting System (IFS) (Flemming et al., 2009) meteorological model. TM5 allows a two-way nesting of regions (Krol et al., 2005), however, the nesting was not applied to the simulations submitted to the intercomparison.

The simulations were conducted with horizontal resolutions of 3° × 2° and 31 vertical layers. The 3-hourly European Centre for Medium-range Weather Forecasts (ECMWF) ERA-Interim reanalysis data (Simmons et al., 2007) were used for the calculation of the atmospheric transport.

The simulated results of ^{137}Cs and ^{131}I were submitted to the intercomparison. The source terms of ^{137}Cs and ^{131}I estimated by the JAEA (Terada et al., 2012) were used. In the simulation, all of the radionuclides were assumed to be removed by wet deposition only. The parameterization of the wet deposition was assumed to be the same as that of the soluble carbon monoxide.

4A.5. Meteorological Research Institute - Passive-tracers Model for radionuclides (MRI-PM/r)

MRI-PM/r (Meteorological Research Institute (MRI) - Passive-tracers Model for radionuclides; MRI-PM/r) is a regional off-line chemistry transport model developed by the Meteorological Research Institute of the Japan Meteorological Agency. The intercomparison of the long-range transport of radionuclides used a regional domain in the Mercator map projection of 107°E-252°E and 3°N – 61°N with 234 ×120 grids, which corresponded to approximately 60 km × 60 km horizontal resolution. The vertical coordinate was a terrain-following coordinate with 13 vertical layers up to 10 hPa. The Advanced Research Weather Research and Forecasting (WRF) model was used to simulate the meteorological field. The U.S. National Center for Environmental Prediction (NCEP) 6 h, 1°×1° final operational global analysis dataset ds083.2 (http://dss.ucar.edu /datasets/ds083.2) was used for the initial and boundary conditions of the WRF and also for the analysis nudging method.

The aerosol module uses a category approach to describe the interaction between radionuclides and environmental species (Kajino and Kondo, 2011) in which the aerosol

particles are grouped into six categories: primary hot particles (PRI), Aitken mode (ATK), accumulation mode (ACM), dust particles (DU), sea-salt particles (SS), and pollen (POL). The aerosol chemical and dynamic processes, such as nucleation, condensation, coagulation and deposition, are calculated based on the modal moment dynamics approach (Kajino and Kondo, 2011; Kajino, 2011). The emission inventory of the environmental species, such as dust, sea-salt, SOx, NOx, and NHx, and the elemental and organic carbon compounds from anthropogenic, biogenic and biomass burning origins were common to Kajino and Kondo (2011). Five percent of the Cs was assumed to form radioactive primary particles (PRI), and the remaining (95%) Cs was assumed to condense onto pre-existing particles (ATK, ACM, DU, SS and POL) with the mass fluxes proportional to the surface area concentrations of each aerosol category. A revised version of the JAEA inventory (Terada et al., 2012) was used for the emissions of ^{134}Cs and ^{137}Cs.

Appendix 4B. Observational data

4B.1. Atmospheric concentrations

To verify the global simulations, measurements of the atmospheric concentrations from the Comprehensive Nuclear Test Ban Treaty Organization (CTBTO) were used in the intercomparison. At the time of the accident at the FDNPP, the CTBTO had set up 64 observation points for particulate radionuclides as well as 27 observatories for radioactive Xenon as part of a standard procedure by the International Monitoring System (IMS) to supervise the manufacture of nuclear weapons and experiments and operation of nuclear facilities (Medici, 2001; CTBTO, 2011; Yonezawa and Yamamoto, 2011). The CTBTO observatories in Japan are located in Gunma and Okinawa, from which measurement information was released after the accident (Yonezawa and Yamamoto, 2011; Center for the Promotion of Disarmament and Non-Proliferation, 2011). Radionuclides were detected in most of the observatories in the Northern Hemisphere; however, they were diluted during transport and the concentration levels have been low outside of Japan. Therefore, they were not considered to have had an impact on the human body.

4B.2. Measurements of depositions

For the comparison of the deposition of radionuclides, observations of ^{131}I, ^{134}Cs, and ^{137}Cs by the RadNet (National Air and Radiation Environmental Laboratory) of the U.S. Environmental Protection Agency (EPA) and National Atmospheric Deposition Program (NADP) (Wetherbee et al., 2012) were used. Wetherbee et al. (2012) indicated that the ^{131}I observed in the USA had the typical features of atmospheric long-range transport and decreased during transportation from the east to west. Moreover, the radioactive material fallout from the accident at the FDNPP found in the U.S. was reported to be larger than the fallout from the Chernobyl accident.

Appendix 5A. Model descriptions for cceanic dispersion model intercomparison

5A.1. CRIEPI

The CRIEPI employed the Regional Ocean Modeling System (ROMS; Shchepetkin and McWilliams, 2005) to simulate the behavior of ^{137}Cs released from the 1F NPP reactors off of Fukushima (Tsumune et al., 2012; 2013). The ROMS is a three-dimensional Boussinesq free-surface ocean circulation model formulated using terrain-following coordinates. The model domain in this study covered the oceanic area off of Fukushima (35°54′N–40°00′N, 139°54′E–147°00′E). The horizontal resolution was 1 km in both the zonal and meridional directions. The vertical resolution of the σ coordinate was 30 layers. The ocean bottom was set at a depth of 1000 m to reduce the computer resources required for the simulation. We used a third-order upwind difference for the advection scheme for both the momentum and tracers and a fourth-order centered difference scheme for the viscosity and diffusivity in the model. The horizontal viscosity and diffusion coefficient were 5.0 m^2 s^{-1}. The vertical viscosity and diffusion coefficient were obtained by a K-profile parameterization (Large et al., 1994). The background value of the vertical viscosity and diffusion coefficient was 10^{-5} m^2 s^{-1}. The model was forced at the sea surface by wind stress and by heat and freshwater fluxes, and their values were acquired by a real-time nested simulation system (Hashimoto et al.,

2010) of the Weather Research and Forecasting model version V3.2.1 (WRF; Skamarock et al., 2008), which is a global spectral model used for numerical weather prediction created by the Japan Meteorological Agency (JMA).

During the simulation, the horizontal currents, temperature, salinity, and sea-surface height along the open boundary were restored to those of the JCOPE2 reanalysis data (JCOPE2, Japan Coastal Ocean Prediction Experiment 2, Miyazawa et al., 2009). The temperature and salinity were nudged by the JCOPE2 reanalysis results to represent mesoscale eddies in the simulation period in the ROMS with a higher resolution. The nudging parameter was 1 d^{-1}. The initial conditions of temperature, salinity, horizontal current velocities, and sea-surface height were set by the JCOPE2 reanalysis output. Previous simulations considered the tidal effect (Tsumune et al., 2012). We subsequently confirmed that the tidal effects on the behavior of ^{137}Cs were small in these simulations. Therefore, we omitted the tidal effect in this study to simplify the model simulation (Tsumune et al., 2013).

We modeled ^{137}Cs as a passive tracer, with its movement into the ocean interior controlled by advection and diffusion (Tsumune et al., 2011). We assumed that the activity of ^{137}Cs in seawater would decrease as a result of radioactive decay because it has a half-life of 30 years. The direct discharge scenario is from Tsumune et al. (2012; 2013); the total amount of radionuclides was 3.5 PBq at the end of June 2011. The spatial and temporal distributions of the atmospheric deposition of ^{137}Cs were estimated by CAMx (ENVIRON, 2009) and described by Hayami et al. (2012) and Tsumune et al. (2013); the total amount of atmospheric deposition was 1.14 PBq in this region for the period from March 11 to April 1, 2011. The release rate to the atmosphere is from Terada et al. (2012); the total amount of radionuclides was 9.0 PBq. In addition, an inflow flux through the boundary was employed in the simulated results by the North Pacific model (Tsumune et al., 2013).

5A.2. GEOMAR

"GEOMAR" is the name of the model used and described in Dietze and Kriest (2012). It is a global configuration of the MOM4 P0d (GFDL Modular Ocean Model v.4, Griffies et al., 2005) z-coordinate, free surface ocean general circulation model. The horizontal configuration is an eddy resolving around Japan and coarser elsewhere. The vertical grid has a total of 59 levels. The bottom topography is interpolated from the ETOPO5 dataset with a 5-min gridded elevation data set from the National Geophysical Data Center (http://www.ngdc.noaa.gov/mgg/fliers/ 93 mgg01.html). We use partial cells, and the

atmospheric forcing consists of (6 hourly) wind stress, heat, and freshwater flux fields derived from the 40 ERA-Interim re-analyses by the European Centre for Medium-Range Weather Forecasts (ECMWF) (Uppala et al., 2005, and many more to follow). In addition to the heat fluxes from the ECMWF, a flux correction restores the sea-surface temperatures (SSTs) with a time scale of 30 days to the monthly mean SSTs derived from a blend of satellite products (C. Rathbone, personal communication, 2006). Sea-surface salinity is restored to the World Ocean Atlas 2005 (Antonov et al., 2006) annual mean climatology with a timescale of 90 days. The vertical mixing of the momentum and scalars is parameterized with the KPP approach of Large et al. (1994). The relevant parameters are (1) a critical bulk Richardson number of 0.3 and (2) a vertical background diffusivity and viscosity of 10^{-5} m^2/s. We also account for the double-diffusive and nonlocal fluxes. The integration starts from rest with initial temperatures and salinities interpolated from the World Ocean Atlas 2005 annual mean (Locarnini et al., 2006; Antonov et al., 2006) onto the model grid. After a spinup of 5 yr that covers the period from 1993 to 1998, the clock assigning the model forcing is reset to 1993, and the model is integrated for another 5 yr. A comparison of the simulated currents with those derived from the satellite altimetry suggests (as shown by Dietze and Kriest, 2012) that our nominal "1993 state" (following the spinup) is similar to the actual conditions during the accident in 2011. Note that this is a pragmatic approach. Ideally, we should have applied actual and realistic fluxes to drive the circulation model. Nonetheless, as a result of uncertainties in the initial conditions and the highly nonlinear dynamics of ocean eddies, an exact hindcast is impossible without constructing a complex data assimilation machinery.

The accidental release of ^{137}Cs is simulated by embedding (online) an artificial tracer into the MOM4 P0d circulation model. The tracer (2.3PBq) is released into a surface grid-box comprised of the 10×10 km grid closest to the location of the nuclear power plant on April 1. The tracer is conservative; therefore, it does not decay but behaves similarly to a dye and is subject to mixing and advection only. For timescales much shorter than the ≈30 yr half-life of ^{137}Cs, the behavior of our artificial tracer mimics that of ^{137}Cs. Because we released all of the ^{137}Cs within one time step into one grid box, in the first days following the release, the numerical dispersions were smoothed until the initial steep spatial gradients. Although this is clearly spurious behavior, we find that the associated fluxes are insignificant when compared to the total release.

5A.3. IRSN

The IRSN used the Model for Application at Regional Scale (MARS3D) (Lazure and Dumas, 2008) to simulate the dispersion of ^{137}Cs released from the FDNPP reactors towards the open sea. The MARS3D is a three-dimensional free-surface ocean circulation model formulated using sigma coordinates. To remain applicable in a "crisis" situation, we use the MARS3D model "as is." This model is usually applied along the European continental shelf in both tidal and thermohaline contexts (Bailly du Bois et al., 2012a; Batifoulier et al., 2012; Garreau et al., 2011). The model domain covers the oceanic area off of Fukushima: 31°N - 43.2°N, 137°E - 150°E (1000 km × 1200 km, Fig. 5.1), and the horizontal resolution is approximately 1.852 km (one nautical mile, 1/60°) in an E-W and N-S direction, with 742 grid cells in the E-W direction and 622 in the N-S direction. The vertical resolution of the sigma coordinate is 40 layers that are refined near the surface. The bathymetric data are derived from the JODC (JODC, 2011). The model accounts for the regional and local circulation, i.e., the Kuroshio Current, flux through the Tsugaru Strait, wind forcing and tides. The tide at the open boundary conditions is described using 16 tidal harmonic components from the FES2004 numerical atlas (Lyard et al., 2006) with a horizontal resolution of 1/8°. At the scale of thermohaline and geostrophic effects, the initial and boundary conditions are derived from the daily oceanic forecast and hindcast of the global model proposed by the MERCATOR-ocean model with a resolution of 1/12° (http://www.mercator-ocean.fr/eng (Ferry et al., 2007)). For the downscaling procedure, the temperature, salinity, currents and sea level are interpolated in both time and space to provide the boundary conditions. Similarly, the wind forcing, water and heat flux are downscaled from the atmospheric forecast and hindcast of the NCEP meteorological global model (http://www.ncep.noaa.gov/) with a resolution of 1/2°.

The ^{137}Cs source term from the direct release is derived from the calculated flux provided in Bailly du Bois et al. (2012b) and amounts to 27 PBq. The atmospheric deposition is calculated from the hourly deposition derived from the atmospheric dispersion calculations using the IRSN's Gaussian puff model pX (Korsakissok et al., 2013), which estimates a total deposition onto the sea of 3 PBq on March 23, 2011.

The initially applied wind drag coefficient (Cd) initially is a classically adopted value with p=0 in Cd=0.0015×Wp. W represents the wind vector module (Wx, Wy) at 10 m. We have fixed p=0.8 to fit with the measured time-evolution of the ^{137}Cs amounts based on hundreds of measurements integrated over space and time in an area of 50 × 100 km facing the FDNPP. We consider that the environmental half-time measured in this area is a robust

parameter for the model comparison. With regards to general circulation, this modification of the drag coefficients does not change the main patterns, such as the position and strength of the Kuroshio Current and generation of eddies and loops; however, it obviously increases the surface current variability.

5A.4. JAEA

An oceanic forecasting system of radionuclide dispersion was developed by the Japan Marine Science Foundation of Kyoto University and the JAEA to predict the radionuclide dispersion associated with a spent nuclear fuel reprocessing plant in Rokkasho Village, Aomori Prefecture. A three-dimensional ocean general circulation model developed at Kyoto University and the Japan Marine Science Foundation calculates the ocean current, temperature, salinity, etc., whereas the oceanic dispersion model SEA-GEARN developed at the JAEA predicts the radionuclide dispersion (Kobayashi et al., 2007). We performed a downscaled calculation from the North Pacific with a horizontal resolution of 1/8° × 1/6° to a finer domain in the northwestern North Pacific with a horizontal resolution of 1/24° × 1/18°. Subsequently, a similar downscale calculation predicted an oceanic condition for a coastal area off of the Fukushima Prefecture with a horizontal resolution of 1/72° in latitude and 1/54° in longitude. The finest model was forced by the data from the National Centers for Environmental Prediction-Department of Energy (NCEP-DOE) Reanalysis 2 and the Mesoscale Model (MSM) wind data constructed at the Japan Meteorological Agency. In addition, a data assimilation with the four-dimensional variational method was adopted to perform a reanalysis in a northwestern region of the North Pacific (Ishikawa et al., 2009). The assimilated data consisted of the satellite altimeter data from the Archiving, Validation, and Interpretation of Satellite Oceanographic data/Collect Localisation Satellites (AVISO/CLS) and sea-surface temperature data from the Operational Sea-Surface Temperature and Sea Ice Analysis (OSTIA), etc.

We used a source term for the ^{137}Cs amount discharged into the ocean that was primarily based on the term estimated by Kawamura et al. (2011). They successfully constructed a source term using the oceanic monitoring data obtained near the northern and southern discharge channels at the FDNPP. The airborne ^{137}Cs amount deposited at the sea surface was calculated using the Worldwide Version of System for Prediction of Environmental Emergency Dose Information (WSPEEDI-II) developed at the JAEA (Terada et al., 2008).

5A.5. JCOPET

The JCOPET is a high-resolution nested coastal ocean model that is based on the Princeton Ocean Model with a generalized sigma-coordinate in the vertical direction (see Guo et al., 2010 and Miyazawa et al., 2012 for more details) and developed for coastal ocean prediction studies for Japan. It has a 1/36° horizontal grid spacing both in latitude and longitude and covers a domain at 28°N-44°N, 125°E-148°E with 46 vertical levels. The JCOPET is nested in a 1/12° resolution JCOPE2 model of the western North Pacific domain, which is also embedded in a coarser Pacific Ocean model. The JCOPE2 incorporates a sophisticated ocean data assimilation scheme that assimilates the satellite sea-surface height anomaly, satellite-observed sea-surface temperature, and in situ temperature and salinity data that are observed by vessels. The required lateral boundary conditions for the JCOPET calculations are derived from these JCOPE2 values. The JCOPET does not possess a data assimilation scheme except for a simple nudging of temperature and salinity towards the JCOPE2 fields; however, the tidal forcing of 16 constituents is imposed at the open boundaries. The freshwater inputs of 35 major rivers within Japan are also considered in the JCOPET calculations. The horizontal mixing coefficients are calculated using a Smagorinsky (1963)-type formula, and the vertical mixing coefficients are derived from a turbulent closure model of Mellor and Blumberg (2004). The surface forcing is obtained by the Japan Meteorological Agency's nonhydrostatic Mesoscale Model (JMA_MSM) with a 5 km resolution.

For the ^{137}Cs dispersion calculation, the velocity fields are obtained from the JCOPET model with the ocean reanalysis output of the JCOPE2 assimilative system (Masumoto et al., 2012). The ^{137}Cs concentrations are dispersed as passive tracers in the JCOPET with a 30.1-year half-life of radioactivity. We adopt both the direct discharge to the ocean from the FDNPP and atmospheric deposition onto the sea surface as source terms of ^{137}Cs for this particular calculation. The direct discharge scenario is similar to the one used by Tsumune et al. (2012), in which the total amount of radionuclides is 5.7 PBq. The spatial and temporal distributions of the atmospheric deposition of ^{137}Cs are estimated by a one-way nested regional air quality forecasting (AQF) system described by Honda et al. (2012), with the total amount of the atmospheric deposition of 0.3 PBq in the western North Pacific for the period from March 11 to May 6, 2011.

5A.6. KIOST/IMMSP

The KIOST/IMMSP is a high-resolution coastal ocean model for radionuclide transport that is based on the finite-element SELFE model (Zhang and Baptista, 2008; Roland et al., 2012). The model was developed by the Korea Institute of Ocean Science and Technology (S. Korea) and the Institute of Mathematical Machine and System Problems (Ukraine). The model domain is 135°-148°E, 32°-43°N with the finest grid resolution close to the FDNPP at approximately 500 m; the total number of elements is 97,989. The vertical coordinate is s-system with 36 s-levels refined near the surface. The vertical viscosity and diffusivity are calculated from the $k-\varepsilon$ model. The surface forcing is obtained from the ERA-Interim reanalysis. The lateral boundary conditions for the KIOST/IMMSP calculations are obtained from the HYCOM nowcast/forecast system. The KIOST/IMMSP temperature is nudged towards the HYCOM fields, and the tidal forcing is imposed at open boundaries using the NAO.99b tidal prediction system.

The Eulerian radionuclide transport model describes the transport of radionuclides in a solution or on suspended sediments and as they settle, resuspend and diffuse into the bottom sediments (Margvelashvily et al., 1997). The sediment (silt) concentration was prescribed, and the liquid release scenario from the FDNPP was adopted from Kawamura et al. (2011); the total amount of ^{137}Cs released was 3.8 PBq.

5A.7. Kobe University

A synoptic, oceanic downscaling based on the UCLA-ROMS (Shchepetkin and McWilliams, 2005) in a double-nested configuration with an Eulerian passive tracer module is developed for the initial oceanic dispersal of dissolved radioactive ^{137}Cs (Uchiyama et al., 2012; Uchiyama et al., 2013). The outer-most boundary condition and initial condition are provided by the assimilative daily-mean JCOPE2 reanalysis (Miyazawa et al., 2009). The 12-hourly averaged solution of the parent ROMS-L1 model at a horizontal resolution of dx = 3 km (256 × 256 × 32) is projected onto the perimeters of the child ROMS-L2 at dx = 1 km (512 × 512 × 32) in time and space with a one-way offline nesting approach (Mason et al., 2010; Buijsman et al., 2012; Romero et al., 2013). Both the L1 and L2 domains are rotated horizontally to approximate an alignment with the coastline of Fukushima Prefecture. A vertically stretched s-coordinate is introduced so that the grid refinement occurs near the surface. Neither the lateral viscosity nor diffusivity is considered other than the intrinsic hyper-diffusion caused by the third-order upwind-biased advection scheme. The KPP model

is used for the surface and bottom planetary boundary layers. The model topography is based on the JODC's J-EGG bathymetry at dx = 0.5 km, which is complemented by the SRTM30 dataset at 30 arc-seconds. An hourly reanalysis of the JMA's assimilative GPV-MSM atmospheric product determines the surface wind stress. The surface heat, freshwater and radiation fluxes and the SSS (with a weak restoring force at a time scale of 90 days) are from the COADS monthly climatology. The monthly climatology of freshwater discharge from all of the major rivers in the model domains is considered as the mass point sources. The online Eulerian tracer tracking is conducted in the L2 model by exploiting the leakage scenario proposed by Tsumune et al. (2012), which ignores the atmospheric fallout and half-life decay of the nuclide. A near-field dilution submodel similar to what is used in Uchiyama et al. (2014) is utilized to avoid underestimating the unresolved dilution near the release site. The relative concentration of ^{137}Cs as a result of the unit leakage flux (1 Bq/s) is computed and then compared to the observed data collected just off of the FDNPP for rescaling to the actual concentration. The L1 model is initialized on Oct. 1, 2010, whereas the L2 model begins on Jan. 1, 2011 to spinup the model ocean sufficiently. The computed circulation, SSH, and ^{137}Cs concentrations are carefully verified against the AVISO satellite altimetry and in situ concentration data of the sampled radionuclides to confirm a reasonable consistency.

5A.8. MSSG

The MSSG is an air-sea-coupled model developed at the JAMSTEC (see Takahashi et al., 2008 for more details). Only the oceanic component is used here. This model has a z-coordinate in the vertical direction and latitude-longitude coordinates in the horizontal direction. The model domain covers and area at 140.2°E-143.2°E and 34.85°N-39.14°N with a resolution of approximately 2 km. The bottom depths are based on the ETOPO1 (Amante and Eakins, 2009) with 73 levels in the vertical direction and a 3 m resolution near the surface. The lateral boundaries of the flow field, temperature, and salinity as well as the surface temperature and salinity are set by the JCOPE2 (Miyazawa et al., 2009). The surface wind stress is estimated based the 10-m wind from the Grid Point Value of Meso-Scale Model (GPV/MSM) from the Japan Meteorological Agency. For the subgrid scale parameterization, a Smagorinsky-type Laplacian viscosity and diffusion are used in the lateral and a Noh-Kim vertical mixing scheme is used in the vertical (Noh and Kim, 1999). There are no freshwater inputs or atmospheric fallout. The model is integrated from Dec. 1, 2010 to June 30, 2011.

A Lagrangian particle-tracking model is used to solve the dispersion of radionuclides (See Choi et al. (2013) for more details). The model simulates the migration of radionuclides between three phases: dissolved in sea-water, adsorbed in large-particulates, and adsorbed in bottom-sediments. Radionuclides are transferred between the sea-water and large-particulates or sea-water and bottom-sediments through adsorption and desorption. Transfers between large-particulates and bottom-sediments occur through settling and erosion, and the radionuclides adsorbed in the bottom sediment are not advected. The oceanic discharge of radionuclides from the FDNPP occurs according to a scenario proposed by Tsumune et al. (2012), which produces a total amount of radionuclide adjusted to 5.5 PBq and assumes that the radionuclides are dissolved in sea water.

5A.9. NIES

An ocean model has been developed by the National Institute for Environmental Studies (NIES) to evaluate and predict pelagic-benthic environments, especially eutrophication phenomena in coastal bays and shallow shelves. The model is composed of the following three sub-models: hydrodynamic, biogeochemical cycle, and bivalve life-cycle (Higashi et al., 2012). In the latest NIES model, the hydrodynamic sub-model consists of hydrostatic-Boussinesq primitive equations solved by the finite difference method in a collocated grid system. The free sea surface is tracked by the volume-of-fluid (VOF) method (Hirt and Nichols, 1981) in a z-level vertical grid. The vertical mixing process is parameterized using the Level 2.5 turbulence-closure model (Mellor, 2001), and the horizontal mixing is calculated according to Smagorinsky (1963). The sea-surface fluxes are the boundary conditions for the momentum and heat transport equations and evaluated using the method of Kondo (1975).

In the NIES simulation, the ^{137}Cs dispersion was obtained by solving an advection-diffusion equation with source/sink terms from the same numerical method as the heat and the salinity transports with 2.2 km horizontal resolution. The source terms included the direct discharge to the ocean from the FDNPP and atmospheric deposition onto the sea surface. The spatial and temporal distributions of the atmospheric deposition of ^{137}Cs were simulated by the WRF-CMAQ model (Morino et al., 2013) with a 3 km horizontal resolution. The time series data of the ^{137}Cs direct discharge was identical to the data estimated by Tsumune et al. (2012). The sink term only considered the radioactive decay, and the current fields were simulated by the hydrodynamic sub-model under the following conditions. For

the atmospheric conditions, we used the surface data (hourly, 5 km resolution) of the wind velocity, air temperature, specific humidity, and air pressure from the grid point value-mesoscale model (GPV-MSM) provided by the Japan Meteorological Agency (JMA). For the downward short-wave and long-wave radiations, we used the grid data (6 hourly, 110 km resolution) produced by the JMA climate data assimilation system (JCDAS). The current field data derived from the FRA-JCOPE2 (Miyazawa et al., 2009) (daily, 1/12° resolution) was applied to the lateral open-boundary conditions and T-S assimilation data (simple nudging). The simulation was completed with the supercomputer at the NIES.

5A.10. WHOI-2D

Observation-based two dimension velocity fields are from the daily near-surface geostrophic currents (on a regular Mercator 1/3°×1/3° grid) from AVISO with 6-hourly Ekman velocities (2°×2° degree) based on the NOAA NCEP/ NCAR wind stresses. The wind stress at a 10 m height, τ, was converted to the ocean velocity at a depth of 15 m, u_{Ek} and v_{Ek}, using the Ralph and Niiler (1999) formula $u_{Ek} + iv_{Ek} = \beta\, e^{-i\theta}/(f\rho)\,(\tau_x + i\tau_y)/\sqrt{|\tau|}$, where ρ = 1,027 $kg \cdot m^{-3}$ is the assumed seawater density, f is the Coriolis parameter, $\theta = 55°$ is the rotation angle of the Ekman current, and $\beta = 0.065\ s^{-1/2}$. This observation-based velocity is reliable and provides global coverage; however, it has sparse temporal and spatial resolution and a two-dimensional nature and lacks ageostrophic components. To account for the lateral diffusion and the influence of the unresolved scales, a small stochastic velocity (of a random sign taken from the normal distribution with a standard deviation of 5 cm s^{-1}) was added to the sum of the geostrophic and Ekman velocities. We have verified that the results of our simulations are not sensitive to the specifics of this stochastic velocity field; however, we have listed these details for thoroughness.

The spread of ^{137}Cs is modeled using a Lagrangian framework by repeatedly releasing large numbers of simulated water parcels inside the source domain over the full duration of the source time series. These water parcels are advected by the velocity fields described above, and their trajectories are estimated using a fixed-step (RK4 for runs with the stochastic velocity component) or variable-step (RK4(5) for runs without the stochastic velocity component) Runge–Kutta integration scheme with a bilinear interpolation in time and space between the grid points. The exponential decay of ^{137}Cs concentrations from the initial source value (half-life of 30.16 years) is applied to estimate the concentration of ^{137}Cs following each water parcel. This Lagrangian model provides an intuitive framework that

illuminates the physical mechanisms by which the contaminated waters are brought from the source region to their position at any given time. The disadvantage of this framework is its numerical intensity, which result from the large number of released water parcels and the simplified method by which the calculation treats the diffusion process. As the number and frequency of the released parcels increases, the resulting Lagrangian distribution of ^{137}Cs approaches the value estimated from an Eulerian calculation with the corresponding value of diffusivity. To validate the process, the results of our simulations were tested to ensure that they were not sensitive to further increases in the number of the released parcels. The lack of sensitivity to such an increase suggests that the observed distribution of ^{137}Cs is close to the limiting value (i.e., for an infinitely number of parcels).

5A.11. WHOI-3D

The ^{137}Cs dispersion calculation was the same as in the WHOI-2D model; however, three dimension velocity fields were from the Navy Coastal Ocean Model (NCOM), a high-resolution numerical model (Barron et al., 2004; 2006). A regional model with a 3 km horizontal resolution was nested with open boundaries within the HYCOM global 1/8° model. The model has a hybrid vertical coordinate system with 15 z-levels at the top and 35 density-defined levels underneath for a total of 50 vertical levels. The model was forced with wind and heat fluxes from the Coupled Ocean/Atmosphere Mesoscale Prediction System for the Western Pacific (COAMPS_WPAC). Tides at the boundaries were provided by the Oregon State Model (Egbert and Erofeeva, 2002). The SSH, SST and available T-S profile data from the Naval Oceanographic Office were assimilated into this model using optimal interpolation. The model was run each day, and the data from the previous day were assimilated to provide a 48-hour forecast. One-day segments at the beginning of each run were then stacked together to create a longer time-series covering the time interval from mid-March until the end of June 2011. There were discontinuities in the velocity field between the end of one day and beginning of the next day; however, these were small and did not create any known issues in our evaluation. Unlike our observation-based circulation, the NCOM 3-D velocities varied with depth throughout the water column and had the advantage of improved spatial and temporal resolution than what was provided by the observations. The disadvantages of the NCOM were the smaller model domain and limited ability to match specifically measured oceanic features, such as the exact position of the Kuroshio Current and mesoscale eddies present during the spring of 2011, with the model estimate of the

circulation field. Compared to the observation-based model, the NCOM generally overestimated the mean Kuroshio Current velocity; however, it slightly underestimated the mean currents throughout the rest of the domain. The general shape of the mean Kuroshio Current was captured relatively well in the NCOM; however, its exact position meandered, and the mesoscale eddies were slightly misplaced in the NCOM compared to observations. The variability in the eddy velocities was of the same order in the two models, with the highest variability in the general area of the Kuroshio extension.

Appendix 5B. Horizontal distribution maps

The 10-day averaged horizontal distributions of ^{137}Cs (surface velocities) for the end of March and April are shown in Figs. 5.4 and 5.6 (Figs. 5.5 and 5.7), respectively, and the general descriptions of the figures are written in the main text. However, to view the details of the similarities and differences among the models in terms of shorter time-scale variations, finer-scale velocity distributions, and associated dispersions of the radionuclides, it is helpful to show all of the 10-day averaged maps for all of the model results. Here, we show a sequence of 10-day averaged maps for the ^{137}Cs and surface velocity distributions from March 22-31 to June 20-29, 2011, including Figures 4 to 7 again for thoroughness.

5B.1. 10-day averaged maps of ^{137}Cs at the sea surface

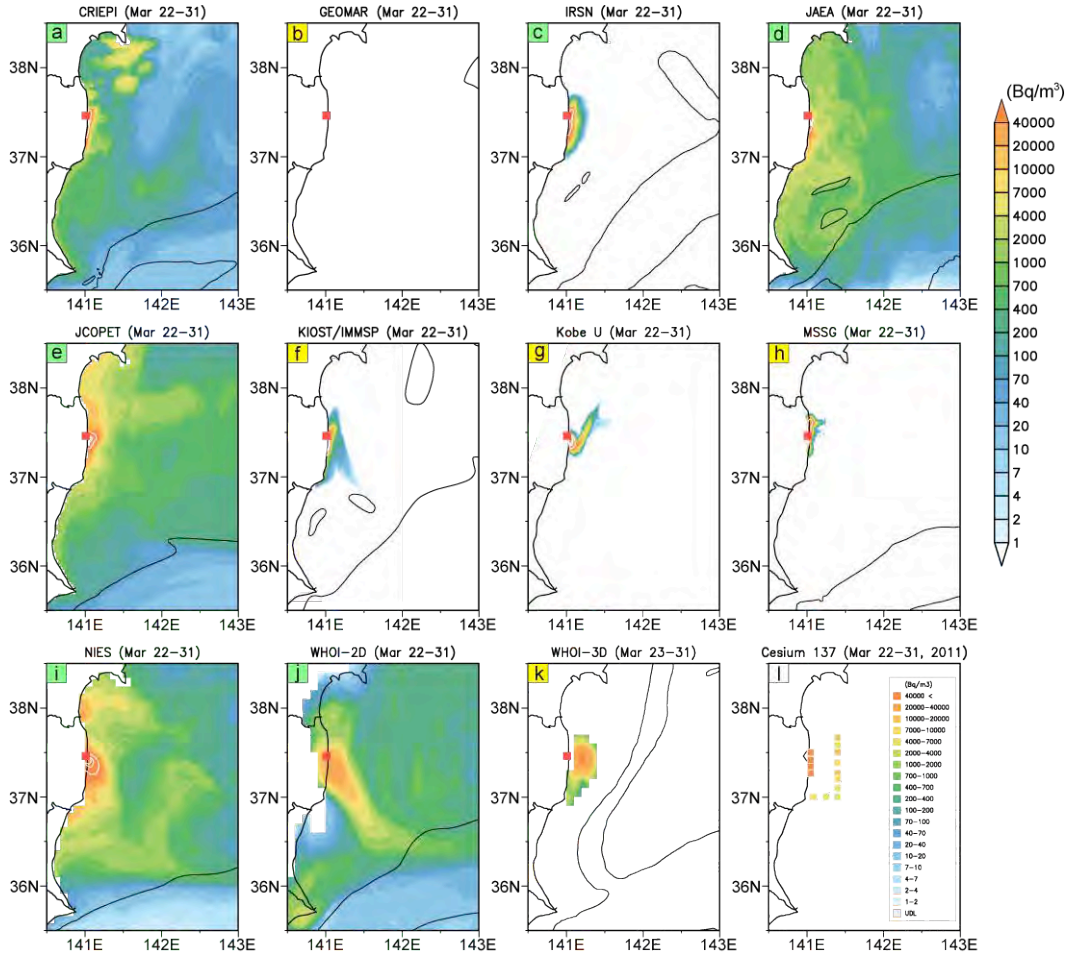

Figure 5B.1. (a)-(j) Horizontal distributions of ^{137}Cs concentration averaged over a 10-day period from March 22 to 31, 2011, with the name of the models indicated above each panel. Red squares indicate the location of the FDNPP. Black thin lines superposed on ^{137}Cs concentration indicate the contours of 0.5 m/s of the surface current magnitude, which show the general locations of the Kuroshio Current and other dominant features in this region. Panels with green (yellow) labels show results from models with (without) atmospheric deposition. Panel (l) shows the distribution of observed ^{137}Cs concentration during the same 10-day period.

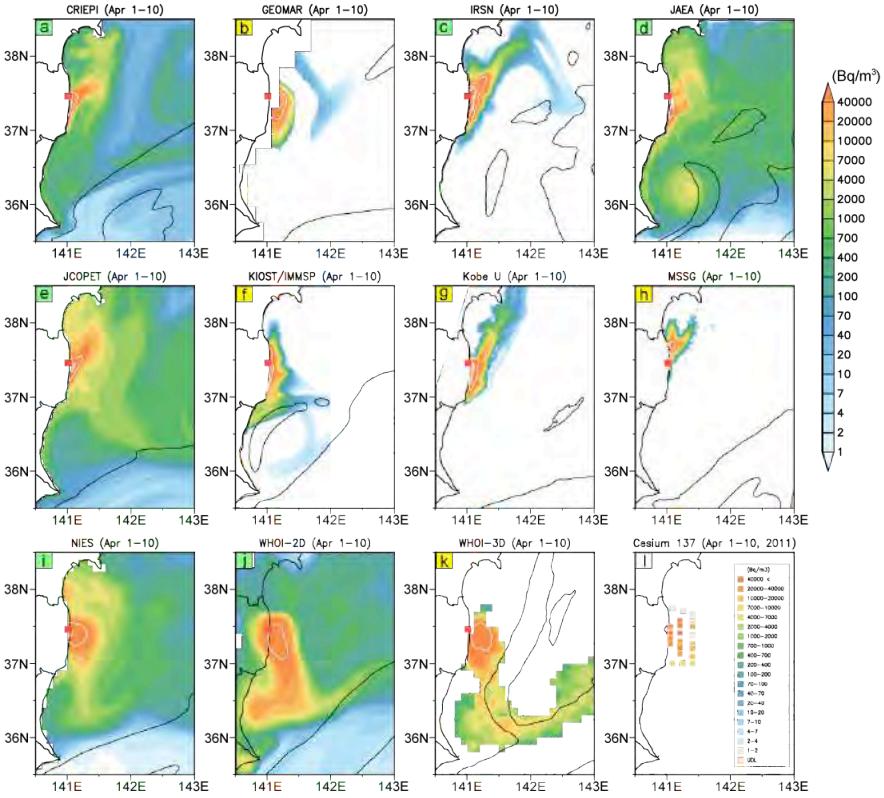

Figure 5B.2. Same as Fig. 5B.1 except for a period between April 1 and April 10.

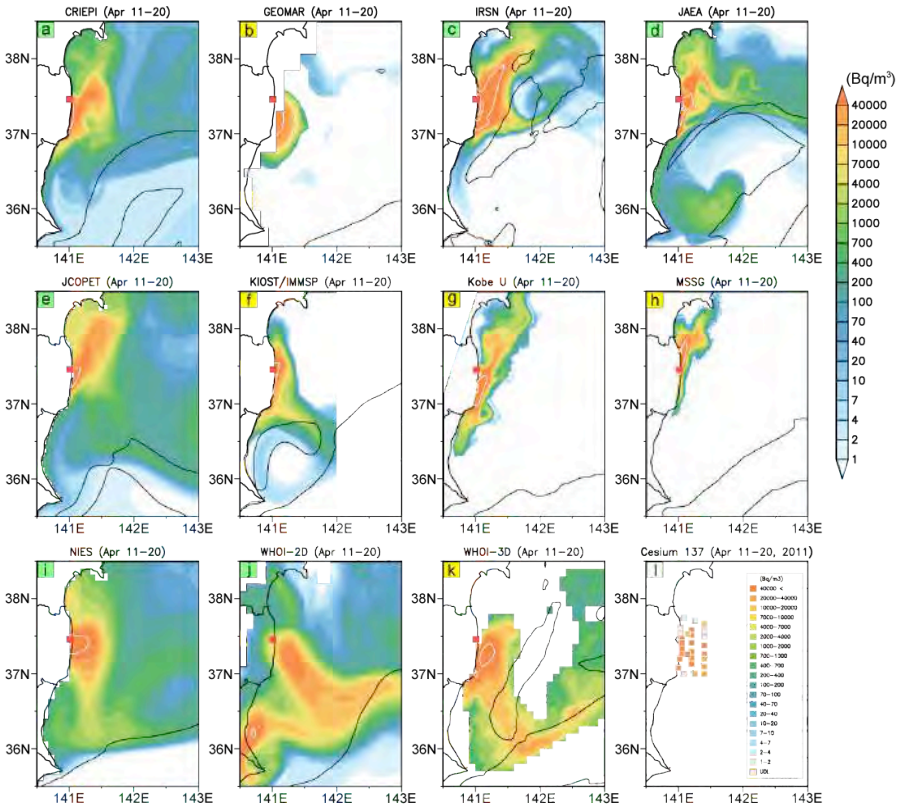

Figure 5B.3. Same as Fig. 5B.1 except for a period between April 11 and April 20.